Makara Journal of Science

Volume 28
Issue 3 *September*

Article 6

9-27-2024

First-Principles Calculations of Thermoelectric Properties of Fe-Based Full- Heusler Fe2CuSi

Ai Nurlaela
Physic Education Departement, Syarif Hidayatullah State Islamic University Jakarta, Jl. Ir H. Juanda No.95, Cempaka Putih, Banten, 15412, Indonesia

Dwi Nanto
Physic Education Departement, Syarif Hidayatullah State Islamic University Jakarta, Jl. Ir H. Juanda No.95, Cempaka Putih, Banten, 15412, Indonesia, dwi.nanto@uinjkt.ac.id

Anugrah Azhar
Department of Physics, Faculty of Science and Technology, Syarif Hidayatullah State Islamic University Jakarta, Jl. Ir H. Juanda No.95, Cempaka Putih, Banten, 15412, Indonesia

Elvan Yuniarti
Department of Physics, Faculty of Science and Technology, Syarif Hidayatullah State Islamic University Jakarta, Jl. Ir H. Juanda No.95, Cempaka Putih, Banten, 15412, Indonesia

Tony Kristiantoro
Research Centre for Electronics, National Research and Innovation Agency, Bandung 40135, Indonesia

First-Principles Calculations of Thermoelectric Properties of Fe-Based Full-Heusler Fe2CuSi

Authors

Ai Nurlaela, Dwi Nanto, Anugrah Azhar, Elvan Yuniarti, Tony Kristiantoro, and Dedi Dedi

Makara Journal of Science, 28/3 (2024), 226-233
doi: 10.7454/mss.v28i3.1469

First-Principles Calculations of Thermoelectric Properties of Fe-Based Full- Heusler Fe_2CuSi

Ai Nurlaela[1], Dwi Nanto[1*], Anugrah Azhar[2], Elvan Yuniarti[2], Tony Kristiantoro[3], and Dedi[3]

1. Physic Education Departement, Syarif Hidayatullah State Islamic University Jakarta, Jl. Ir H. Juanda No.95, Cempaka Putih, Banten, 15412, Indonesia
2. Department of Physics, Faculty of Science and Technology, Syarif Hidayatullah State Islamic University Jakarta, Jl. Ir H. Juanda No.95, Cempaka Putih, Banten, 15412, Indonesia
3. Research Centre for Electronics, National Research and Innovation Agency, Bandung 40135, Indonesia

[*]*E-mail: dwi.nanto@uinjkt.ac.id*

Received November 23, 2023 | Accepted July 8, 2024

Abstract

A first-principle study using density functional theory (DFT) and Boltzmann transport was conducted to evaluate the thermoelectric (TE) properties of an Fe-based full-Heusler alloy. The compound studied is Fe_2CuSi with a Cu_2MnAl-type structure. The electronic properties of Fe_2CuSi were obtained using DFT calculations by running the Quantum ESPRESSO (QE) package. By contrast, TE properties, including electron thermal conductivity, electric conductivity, and Seebeck coefficient, were computed using a semi-empirical Boltzmann transport model solved through the BoltzTraP software at 50–1,500 K temperature range. The spin-orbit coupling effect on these properties was also evaluated, demonstrating notable effects on the results. Multiple electronic bands crossing the Fermi level for both spin directions were confirmed by the density of state curve, indicating the metallic behavior of Fe_2CuSi. The magnitude of the figure of merit was determined by the Seebeck coefficient, electric conductivity, and electron thermal conductivity. In this study, the maximum dimensionless figure of merit was 0.027, reached at 1,000 K for the spin-down channel.

Keywords: density functional theory (DFT), electrical conductivity, Seebeck coefficient, thermal conductivity, thermoelectric

Introduction

Although Cu, Mn, and Al showed no magnetism at room temperature in 1903, Heusler compounds have been known since Friedrich Heusler announced the discovery of ferromagnetic properties of Cu_2MnAl at room temperature [1]. In recent years, the Heusler compound family has gained considerable interest from the scientific community, emerging as a focal point of research in material science and condensed matter physics due to their unique electronic and magnetic properties [2, 3]. Furthermore, Heusler compounds introduce an extensive field for distinctive arrangements due to their tunable materials and broad range of designs [4]. As one of the most prominent families of Heusler alloys, a full-Heusler has a chemical arrangement of X_2YZ, where *transition metals occupy X and Y*, and *the main group element occupies Z*. This alloy commonly exhibits faced-centered cubic crystal structure. According to how atoms occupy the four Wyckoff positions, two types of full-Heusler structures are available. The Cu_2MnAl-type structure is also called the *L*21-type with space group (No. 225), and the Hg_2CuTi-type structure is also known as the *XA*-type with space group (No. 216). In the *L*21 structure, *X* atoms occupy the 8c (¼, ¼, ¼) site, whereas the *Y* and *Z* atoms occupy the 4b (½, ½, ½) and 4a (0, 0, 0) sites, respectively. By contrast, in the *XA* structure, the *X* and *Z* atoms occupy the 4d (¾, ¾, ¾) and 4a (0, 0, 0) sites, respectively, and the *X*' atoms occupy the 4b (½, ½, ½) site [3].

Considering its high tuning capability, theoretical and experimental research on its full-Heusler properties, such as electronic, magnetic, optic, and thermoelectric properties, have been extensively conducted. Each property of full- Heusler compounds allows for its application in some technology, such as shape memory materials, spintronics, and thermoelectric devices [2–5]. This study, focused on electronic and thermoelectric properties because the properties of the material have attracted considerable interest from researchers to find suitable materials for thermoelectric power and spintronics applications. The material is first designed and simulated computationally and theoretically using

the density functional theory (DFT) method before its synthesis to obtain the desired full-Heusler material with a suitable property for any application. The most crucial parameter to determine the performance of a thermoelectric device is the dimensionless figure of merit, *ZT*, which is expressed as [3, 6].

$$ZT = \frac{S^2 \sigma \tau}{K} \quad (1)$$

where *S, T, σ,* and *k* are the Seebeck coefficient, temperature, electrical conductivity, and thermal conductivity, respectively; $K = K_e + K_l$ with K_e and K_l are the electronic and lattice thermal conductivities, respectively [6]. According to the above equation, the Seebeck coefficient, electrical conductivity, and thermal conductivity will determine the value of the figure of merit. A high Seebeck coefficient and electrical conductivity are required to maximize the *ZT*. By contrast, thermal conductivity must be low [7]. Several researchers have conducted investigations to find materials with these characteristics. Balke *et al.* found that the *ZT* max of Co_2MnSi is 0.039, obtained at temperatures above 900 K [8]. Barth *et al.* [9] revealed that the *ZT* max value is higher than that of Co_2TiSn (0.033 at 370–400 K), Mondal *et al.* [10] found *ZT* max values of the semi-metallic full-Heusler compound (0.0052 at 300 K for Ru_2NbAl) and Ramachandran *et al.* obtained a value of 0.0027 at 300 K for $Ru_2VAl_{0.25}Ga_{0.75}$ [11].

Thermoelectric power generation has been explored as an environmental technology, but certain prominent thermoelectric materials incorporate rare, expensive, and environmentally hazardous elements. Fe-based full-Heusler alloys have received considerable attention because they are eco-friendly, earth-abundant, and inexpensive [12]. Hanada *et al.* found excellent thermoelectric properties in the Fe_2VAl compound, revealing the first Fe-based full-Heusler with a 0.2 *ZT* value [13]. Their work motivated other researchers to find Fe-based full-Heusler thermoelectric materials. The reported work on the first-principle of Fe-based Heusler alloys, namely Fe_2TiSn and Fe_2TiSi, which were obtained from DFT calculations within the generalized gradient approximation (GGA), reached the *ZT* values of 0.6 when the k value was less than 3.0 $Wm^{-1}K^{-1}$ with the electron carrier concentration of 4.0 x 10^{20} cm^3. These *ZT* values are substantially higher than 0.2 in previously reported Fe_2VAl-based alloys [14]. Another study reported that the transport calculations of $Fe_{2+x}V_{1-x}Al$ based on the Boltzmann theory yield high values (up to 0.75) of *ZT*, reached when $x = 0.25$ and $x = 0.50$ [15]. Meanwhile, the first-principle calculation on Fe_2MnSi using the approximation methods GGA + U shows that *ZT* is linearly proportional to the temperature, revealing a notable increase in value from 9.15472×10^{-4} at 100 K to 9.16×10^{-2} at 800 K [6]. Reports on the Fe_2CuSi compound are currently unavailable. The information on the first-principle calculations of the thermoelectric of Fe_2CuSi may be necessary for the following experimental activities to consider their research goal. Previous work showed the Fe_2CuSi has dynamic stability with a stable structure that of *L*21 [16].

Research on he first-principle of Fe_2CuSi aims to obtain thermoelectric properties, including the electrical conductivity, electronic thermal conductivity, and the Seebeck coefficient, which were computed using a Boltzmann semi-empirical transport model solved through the BoltzTraP software at the temperature range of 50–1,500 K. Iron has abundant, eco-friendly and inexpensive characteristics. The composition of Fe_2CuSi may be necessary for any application, such as shape memory materials, spintronics, and thermoelectric devices.

Methods

The calculations used a methodology based on DFT calculations and Boltzmann transport theory. The DFT calculation was initially employed to optimize the structure of the Fe_2CuSi material by operating the QE collection, and the electron transport properties, including Seebeck coefficient, electrical conductivity, and electronic thermal conductivity, were calculated using the semi-classical Boltzmann transport approach implemented in the BoltzTraP package [17]. DFT is a quantum mechanical approach to matter based on the Kohn-Sham equation (the mathematical equation of Schrodinger) as an energy-searching method using charge density [18]. Among researchers, Quantum ESPRESSO is useful for electronic-structure calculations and material modeling based on DFT, plane waves, and pseudopotentials [19]. Simultaneously, BoltzTraP software is used to calculate the thermoelectric properties of the material. This program calculates the smoothed Fourier expression of the periodic function and semi-classical transport coefficients for an extended system using the linearized Boltzmann transport equation [20]. Thermoelectric criteria were calculated with a constant relaxation time estimation $\tau = 10^{-14}$ s, commonly used in similar calculations [6]. The wave function kinetic energy cutoff was set to 75 Ry for all calculations.

Therefore, in this work, the atomic positions of Fe, Cu, and Si correspond to the atomic positions of Cu, Mn, and Al for the Cu_2MnAl structure, respectively. The 8c (¼, ¼, ¼) site is occupied by Fe atoms, whereas the 4b (½, ½, ½) and 4a (0, 0, 0) sites are occupied by Cu and Si atoms, respectively. This finding is consistent with Gu et al., in which the ground-state of Fe_2CuSi was found at an *L*21-type structure with a ferromagnetic configuration and a lattice constant of 5.578 Å. Figure 1 shows XCrySDen visualization of the crystal structure of Fe_2CuSi with the aforementioned atomic positions. This structure was obtained through self-consistent field (SCF) calculation on a k-point grid mesh. Electronic

properties, including band structure and density of state (DOS) for the system, were calculated through the SCF calculation with a 121212 k-point grid mesh. Instead, the k-point grid mesh was densed into 202020 to obtain a precise chemical potential value in the NSCF calculation. Meanwhile, a smooth band structure was acquired with the NSCF calculation on the k-point grid mesh and 20 k-points along the k-path. The convergence threshold is 1×10^{-6} for calculations of SCF, NSCF, and bands.

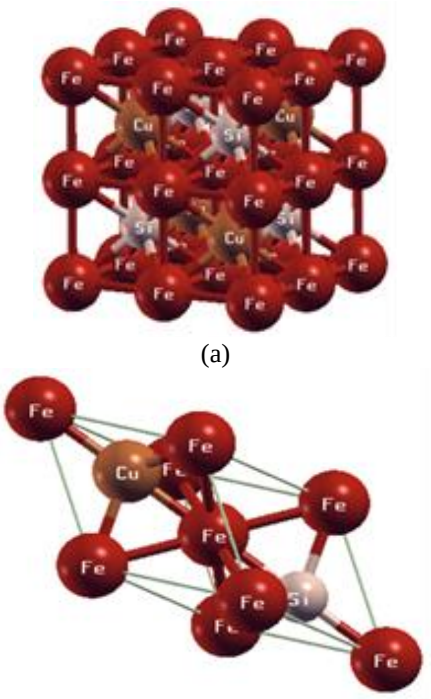

(a)

(b)

Figure 1. (a) Conventional Unit Cell and (b) Primitive Unit Cell of Fe2CuSi

Results and Discussion

Electronic properties. The electronic properties of the full-Heusler compound Fe_2CuSi were investigated. The examination was based on the established ground state structure and the equilibrium lattice. The ground-state structure demonstrates the lowest energy state of the compound at absolute zero temperature. The lattice parameters at the equilibrium state, are called equilibrium lattices, in which the forces within the crystal are balanced. These ground-state structures and equilibrium lattices are crucial for understanding the fundamental electronic properties of the material. The spin-polarized band structures were computed and displayed in Figure 2. As shown in the figure, the Fermi energy was shifted to 0 eV. Notably, It can be seen that only the electronic band structures around the Fermi level have been displayed. The band structure curve in Figure 2 reveals multiple electronic bands crossing the Fermi level in both spin directions, exibithing the metallic behavior of Fe_2CuSi in the Cu_2MnAl-type structure, which is substantially close to the computational result reported by Gu *et. al* [16]. Previous research found differences in this band structure pattern due to variations in band path selection. In this study, the band path selection is Γ, X, W, K, and Γ. By contrast, Gu *et al.* chose the band path selections W, L, X, W, and K. The DOS curve in Figure 3 verified the band structure results; an energy band gap is absent, contributing to the metallic features of these compounds [6, 16].

Thermal and electrical conductivity. The electron thermal conductivity, electrical conductivity, and Seebeck coefficient measurements are obtained by inputting the results of electronic structure calculations by QE into the BoltzTraP package. A Fourier expansion scheme was used in the BoltzTraP package to cohere the electronic structure for transport property calculations [21]. The electronic transport behaviors were placed in a temperature range of 50 K to 1,500 K. Figure 4 shows the temperature-dependent electron thermal conductivity of the Fe_2CuSi system for spin-up and spin-down channels

The value of $\frac{K_e}{\tau}$ for the spin-up and spin-down channels increases with the temperature. Thermal conductivity shows that thermal energy in motion can traverse the material under a temperature gradient. K comprises the following of two contributions: the electron and lattice parts $(K = K_e + K_l)$. BoltzTraP still focuses on calculating electronic thermal conductivity and only indirectly calculates lattice thermal conductivity. Electric current and heat transfer in metals are primarily carried by electrons. Therefore, the conductivities of metals depend on the number of free electrons that are available to flow through the metal. As displayed in Figure 4, the dependence of electron thermal conductivity on temperature represents the metallic properties; the increasing temperature raises the number of charge carriers (electrons) [22]. Figure 4 shows the linear dependence of electron thermal conductivity for the spin-down channel on the temperature across all temperature ranges of 50 K–1,500 K, while that for the spin-up channel on temperature occurs in the temperature range of 50 K- 500 K; afterward, the thermal conductivity rapidly increases until 1,500 t The value of $\frac{K_e}{\tau}$ for the spin-down channel is smaller than the spin-up one at the temperature of 500 K until 1,500 K.

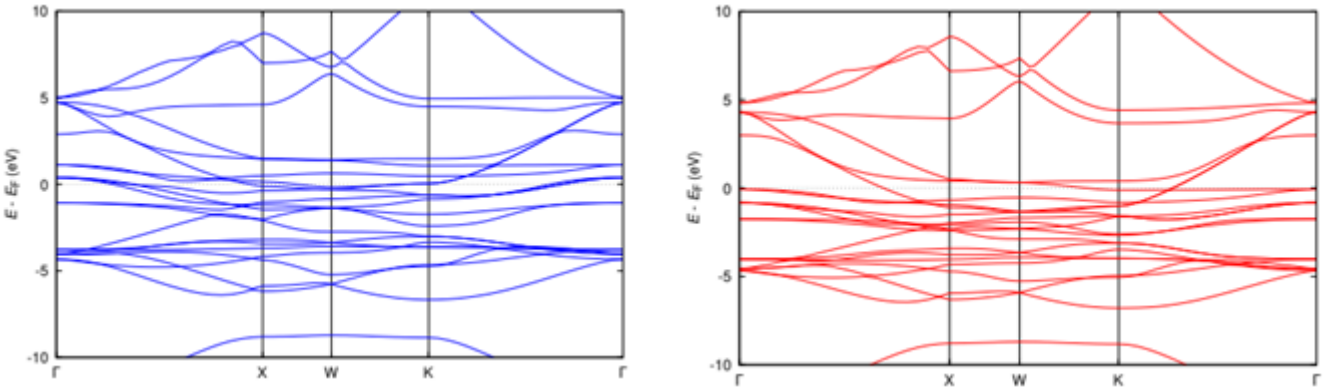

(a) (b)

Figure 2. Band Structure of Fe_2CuSi ($Fm\bar{3}m$): (a) Spin-Up Channel and (b) Spin-Down Channel

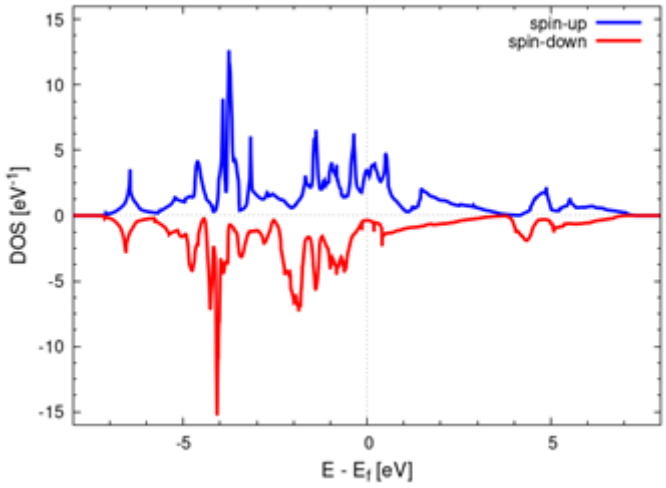

Figure 3. Spin-Dependent Total Density of States or DOS of Fe_2CuSi ($Fm\bar{3}m$)

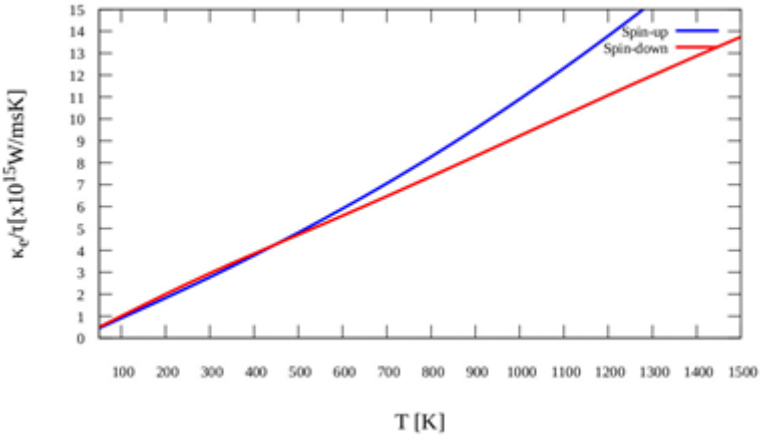

Figure 4. Temperature-Dependent Electron Thermal Conductivity ($\frac{K_e}{\tau}$) of Fe_2CuSi ($Fm\bar{3}m$))

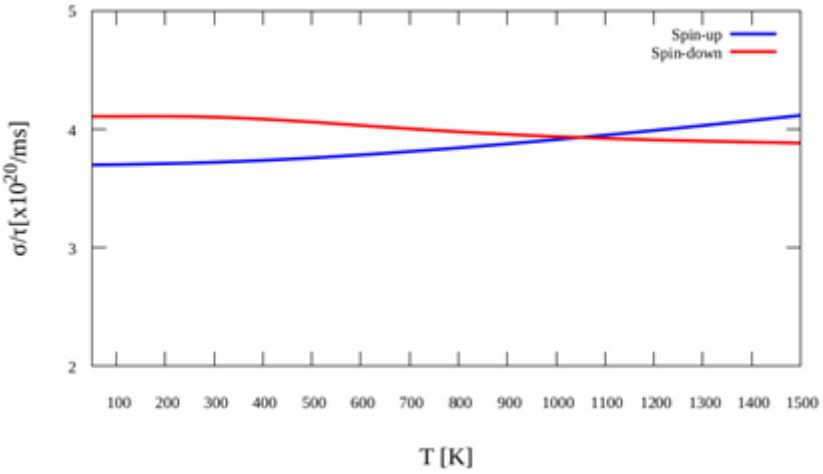

Figure 5. Temperature-Dependent Electrical Conductivity ($\frac{\sigma}{\tau}$) of Fe_2CuSi ($Fm\bar{3}m$)

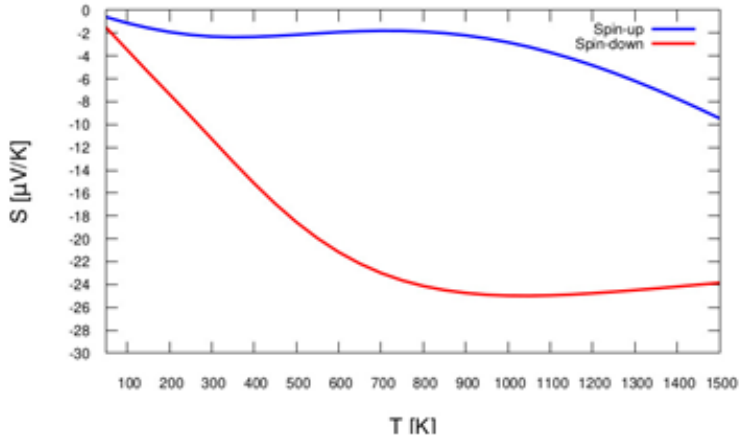

Figure 6. Temperature-Dependent Seebeck Coefficient (*S*) of Fe_2CuSi ($Fm\bar{3}m$)

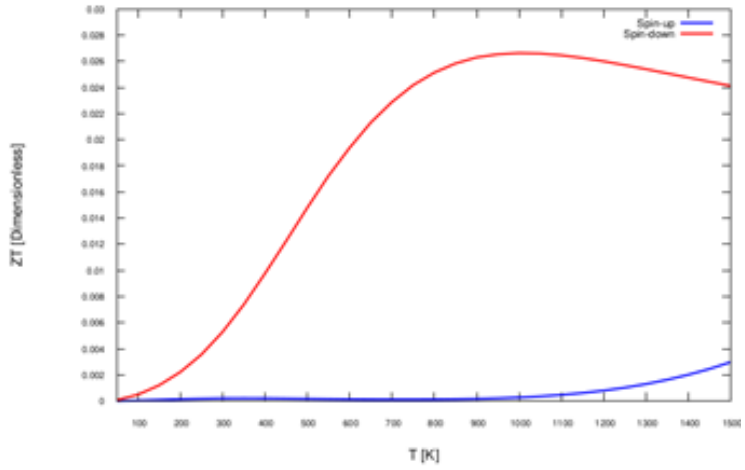

Figure 7. Temperature-Dependent Figure of Merit (*ZT*) of Fe_2CuSi ($Fm\bar{3}m$)

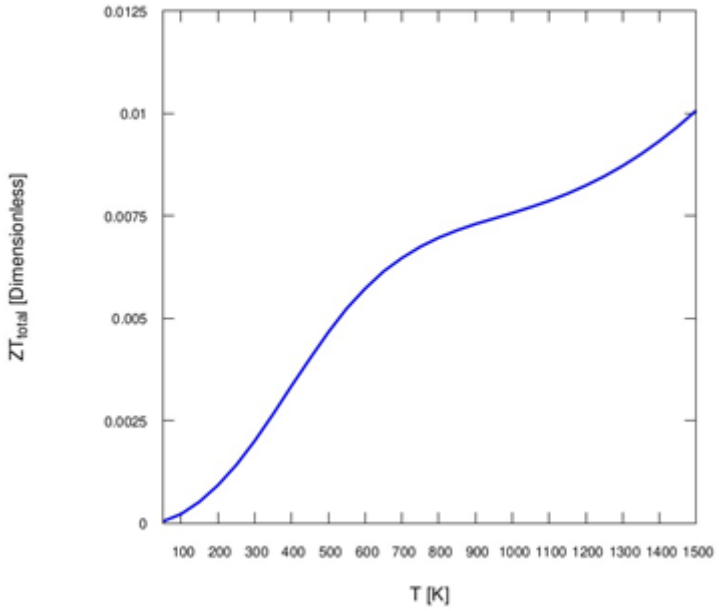

Figure 8. Temperature-Dependent Total Figure of Merit (*ZT*) of Fe_2CuSi ($Fm\bar{3}m$)

Figure 5 shows the temperature-dependent electrical conductivity (σ) per relaxation time τ. The value of $\frac{\sigma}{\tau}$ for the spin-up channel of Fe_2CuSi increases with temperature. By contrast, the value of $\frac{\sigma}{\tau}$ for the spin-down channel decreases as the temperature increases. These results indicate that even in high-temperature regimes, both systems demonstrate electric values with excellent conductivity. The values of $\frac{\sigma}{\tau}$ for the spin-down channel are higher than those for the spin-up channel at temperatures 50 K- 1,000 K, while those for the spin-up channel are higher than those for the spin-down channel at temperatures above 1,000 K until 1,500 K

Seebeck coefficient and figure of merit. The Seebeck coefficient measures the response of a material to a temperature gradient in terms of electric voltage generation. This coefficient directly involves the distribution of electrons near the Fermi level. The energy distribution of electrons near the Fermi level strongly influences the Seebeck coefficient (Figure 6). The calculation results show a different trend for spin-up channels than other ones. *S* increases from 50 K for the spin-up channel, forming a valley around 350 K, and then decreases to establish a peak at 700 K and then increases again until 1,500 K. By contrast, for the spin-down channel, *S* continuously increases from 50 K, forming a valley around 1,050 K, and then decreases until 1,500 K. Notably, *S* is negative for both curves in the entire temperature range, which proposes the electrons as the major charge carriers [6]. The maximum values of *S* for the spin-up and spin-down channels are -9.47 and -25 μVK^{-1} at 1,500 and 1,050 K, respectively. The Seebeck coefficient value of the spin-down channel is 2.6 times higher than that of the spin-up one. These results also agree with the previous study, where the contribution of *S* from the spin-down channel is almost two factors more significant than the one from the spin-up channel [23]. Patel et al. also reported that the Seebeck coefficient for the spin-down channel was higher than that for the spin-up, revealing Seebeck coefficient values of -36 and 180 μVK^{-1} for the spin-up and spin-down channels, respectively, at room temperature (300 K) [24].

Figure 7 shows the temperature-dependent figure of merit (*ZT*) of Fe_2CuSi. *ZT* values are obtained by inputting the Seebeck coefficient (*S*), electron thermal conductivity ($\frac{K_e}{\tau}$), and electrical conductivity ($\frac{\sigma}{\tau}$) at each temperature from 50 K to 1,500 K into Equation 1. The $\frac{\sigma}{\tau}$ values of the spin-down channel are higher than those of the spin-up channel at temperatures 50 K–1,000 K. Meanwhile, the value of the κ_e spin-down channel is smaller than the spin-up channel at a temperature of 400 K until 1,500 K, indicating that the *ZT* values of the spin-down channel are higher than those of the spin-up channel. The *ZT* value of the spin-down channel increases with temperature from 9.40×10^{-5} at 50 K to 0.027 at 1,000 K and decreases after 1,000 K. Maximum *ZT* of around 0.027 is reached at 1,000 K. Elkrimi et al. reported a similar result for the Fe_2MnSi compound, in which *ZT* increases with temperature, revealing a substantial increase in value from 9.15472×10^{-4} at 100 K to 9.16×10^{-2} at 800 K. The *ZT* total was also calculated using the equation below [25].

$$ZT_{total} = \frac{\sigma_{total} S_{total}^2 T}{K_{total}} \quad (2)$$

where

$$\sigma_{total} = \sigma_{\uparrow} + \sigma_{\downarrow} \quad (3)$$

$$K_{total} = K_{\uparrow} + K_{\downarrow} \quad (4)$$

and

$$S_{total} = \frac{\sigma_{\uparrow} \sigma S_{\uparrow} + \sigma_{\downarrow} S_{\downarrow}}{\sigma_{\uparrow} + \sigma_{\downarrow}} \quad (5)$$

Figure 8 shows the *ZT* total of the system for all temperatures from 50 K to 1,500 K. The contribution of the Seebeck coefficient (*S*) from the spin-down channel is higher than *S* from the spin-up channel. Similarly, the *ZT* of the spin-down channel provides an additional contribution to the *ZT* total. The maximum *ZT* total is 0.01, which was reached at 1,500 K.

Conclusion

The thermoelectric properties of full-Heusler compound Fe_2CuSi were investigated based on the first principle DFT. The structural optimization yielded a stable structure, and Fe_2CuSi was regular in the Cu_2MnAl structure. Electronic properties from the band structure and DOS were calculated, revealing the metallic features of the material. The thermoelectric properties of the compound were calculated using DFT and the Boltzmann transport model. The results revealed that spin-dependent thermoelectric properties include electron thermal conductivity, electrical conductivity, and the Seebeck coefficient. For calculated temperatures from 50 K to 1,500 K, *S* was negative with a maximum value of - 9.47 μVK^{-1} at 1,500 K for the spin-up channel and - 25 μVK^{-1} at 1,050 K for the spin-down channel, which proposes the electrons as the major charge carriers. The maximum *ZT* of around 0.027 was reached at 1,000 K for the spin-down channel, which provides additional contributions to the *ZT* total with a maximum *ZT* total of 0.01 at a temperature 1,500 K.

Acknowledgment

This work is funded by BOPTN UIN Syarif Hidayatullah Jakarta UN.01/KPA/223/2022.

References

1 Everhart, W., Newkirk, J. 2019. Mechanical properties of Heusler alloys. Heliyon. 5(5): e01578, https://doi.org/10.1016/j.heliyon.2019.e01578.

2 Beretta, D., Neophytou, N., Hodges, J.M., Kanatzidis, M.G., Narducci, D., Martin-Gonzalez, M., *et al*. 2019. Thermoelectrics: From history, a window to the future. Mater. Sci. Eng. R.-Reports. 138: 100501, https://doi.org/10.1016/j.mser.2018.09.001.

3 Graf, T., Felser, C., Parkin, S.S.P. 2011. Simple rules for the understanding of Heusler compounds. Progress in Solid State Chemistry. 39(1): 1–50 https://doi.org/10.1016/j.progsolidstchem.2011.02.001.

4 Wollmann, L., Nayak, A.K., Parkin, S.S.P., Felser, C. 2017. Heusler 4.0: Tunable materials. Annu. Rev. Mater. Res. 47: 247–270, https://doi.org/10.1146/annurev-matsci-070616-123928.

5 Graf, T., Felser, C., Parkin, S.S.P. 2015. Heusler Compounds: Applications in Spintronics. In Yongbing Xu, David D. Awschalom, Junsaku Nitta. (eds.), Handbook of Spintronics, 1st ed. Springer Dordrecht. Germany. pp. 335–364.

6 El Krimi, Y., Masrour, R., Jabar, A., Labidi, S., Bououdina, M., Ellouze, M. 2020. Structural, electronic, magnetic and thermoelectric properties of Full-Heusler Fe_2MnSi: Ab initio calculations. Results Phys. 18: 103252, https://doi.org/10.1016/j.rinp.2020.103252.

7 Han, C., Li, Z., Dou, S. 2014. Recent progress in thermoelectric materials. Chinese Sci. Bull. 59: 2073–2091, https://doi.org/10.1007/s11434-014-0237-2.

8 Balke, B., Ouardi, S., Graf, T., Barth, J., Blum, C.G.F., Fecher, G.H., *et al*. 2010. Seebeck coefficients of half-metallic ferromagnets. Solid State Commun. 150(11–12): 529–532, https://doi.org/10.1016/j.ssc.2009.10.044.

9 Barth, J., Gerhard, H.F., Benjamin, B., Siham, O., Tanja, G., Claudia, F., *et al*. 2010. Itinerant half-metallic ferromagnets Co_2TiZ (Z=Si, Ge, Sn): Ab initio calculations and measurement of the electronic structure and transport properties. Phys. Rev. B. 81(6): 1–20, https://doi.org/10.1103/PhysRevB.81.064404.

10 Mondal, S., Mazumdar, C., Ranganathan, R., Alleno, E., Sreeparvathy, P.C., Kanchana, V., *et al*. 2018. Ferromagnetically correlated clusters in semimetallic Ru_2NbAl Heusler alloy and its thermoelectric properties. Phys. Rev. B. 98: 205130, https://doi.org/10.1103/PhysRevB.98.205130.

11 Ramachandran, B., Lin, Y. H., Kuo, Y. K., Kuo, C. N., Gippius, A.A., Lue, C.S. 2018. Thermoelectric properties of Heusler-type $Ru_2VAl_{1-x}Ga_x$ alloys. Intermetallics. 92: 36–41, https://doi.org/10.1016/j.intermet.2017.09.012.

12 Bharwdaj, A., Jat, K.S., Patnaik, S., Parkhomenko, Y.N., Nishino, Y., Khovaylo, V.V. 2019. Current research and future prospective of iron-based heusler alloys as thermoelectric materials. Nanotechnol. Russia. 14: 281–289, https://doi.org/10.1134/S1995078019040049.

13 Hanada, Y., Suzuki, R.O., Ono, K. 2001. Seebeck coefficient of $(Fe,V)_3Al$ alloys. J. Alloy. Compd. 329(1–2): 63–68, https://doi.org/10.1016/S0925-838 8(01)01677-2.
14 Yabuuchi, S., Okamoto, M., Nishide, A., Kurosaki, Y., Hayakawa, J. 2013. Large seebeck coefficients of Fe_2TiSn and Fe_2TiSi: First-principles study. Appl. Phys. Express. 6: 025504, https://doi.org/10.756 7/APEX.6.025504.
15 Rai, D.P., Sandeep, Shankar, A., Khenata, R., Reshak, A.H., Ekuma, C.E., *et al*. 2017. Electronic, optical, and thermoelectric properties of $Fe_{2+x}V_{1-x}Al$. AIP Adv. 7: 045118, https://doi.org/10.1063/1.4982 671.
16 Gu, Q., Ji, J., Guo, F., Chen, H., Yang, T., Tan, X. 2021. First principle study on the electronic, magnetic and phase stability of the full-heusler compound Fe_2CuSi. Spin. 11(01): 2150001, https://doi.org/10.1 142/S2010324721500016.
17 Madsen, G.K.H., Singh, D.J. 2006. BoltzTraP. A code for calculating band-structure dependent quantities. Comput. Phys. Commun. 175(1): 67–71, https://doi.org/10.1016/j.cpc.2006.03.007.
18 Hasnip, P.J., Refson, K., Probert, M.I.J., Yates, J.R., Clark, S.J., Pickard, C.J. 2014. Density functional theory in the solid state. Philos. T. R. Soc. A. 372: 20130270, https://doi.org/10.1098/rsta.2013.0270.
19 Giannozzi, P., Baseggio, O., Bonfà, P., Brunato, D., Car, R., Carnimeo, I., *et al*. 2020. Quantum ESPRESSO toward the exascale. J. Chem. Phys. 152: 154105, https://doi.org/ 10.1063/5.0005082.
20 Yaseen, M.S., Murtaza, G., Murtaza, G. 2020. Theoretical investigation of the structural stabilities, optoelectronic and thermoelectric properties of ternary alloys $NaInY_2$ (Y = S, Se and Te) through modified Becke-Johnson exchange potential. Int. J. Mod. Phys. B. 34(13), https://doi.org/10.1142/S02 17979220501337.
21 Witting, I.T., Chasapis, T.C., Ricci, F., Peters, M., Heinz, N.A., Hautier, G., *et al*. 2019. The thermoelectric properties of bismuth telluride. Adv. Electron. Mater. 5(6): 1800904, https://doi.org/1 0.1002/aelm.201800904.
22 Yadav, S.K., Vasu, V. 2016. Synthesis and characterization of copper nanoparticles, using combination of two different sizes of balls in wet ball milling. Int. J. Emerg. Tr. Sci. Technol. 03(04): 3795–3799, https://doi.org/10.18535/ijetst/v3i04.07.
23 Comtesse, D., Geisler, B., Entel, P., Kratzer, P., Szunyogh, L. 2014. First-principles study of spin-dependent thermoelectric properties of half-metallic Heusler thin films between platinum leads. Phys. Rev. B. 89: 094410, https://doi.org/10.1103/PhysRe vB.89.094410.
24 Patel, P.D., Pandya, J.B., Shinde, S.M., Gupta, S.D., Narayan, S., Jha, P.K. 2020. Investigation of full-heusler compound Mn_2MgGe for magnetism, spintronics and thermoelectric applications: DFT study. Comput. Cond. Matt. 23: e00472, https://doi.org/10.1016/j.cocom.2020.e00472.
25 Cahaya, A.B., Tretiakov, O.A., Bauer, G.E.W. 2015. Spin seebeck power conversion. IEEE T. Magn. 51(9): 1–14, https//doi.org/10.1109/TMAG.2015.2 436362.